

NJC

Accepted Manuscript



This article can be cited before page numbers have been issued, to do this please use: M. Ozdemir, D. Choi, Y. Zorlu, B. Cosut, H. Kim, C. Kim and H. Usta, *New J. Chem.*, 2017, DOI: 10.1039/C7NJ00266A.



This is an Accepted Manuscript, which has been through the Royal Society of Chemistry peer review process and has been accepted for publication.

Accepted Manuscripts are published online shortly after acceptance, before technical editing, formatting and proof reading. Using this free service, authors can make their results available to the community, in citable form, before we publish the edited article. We will replace this Accepted Manuscript with the edited and formatted Advance Article as soon as it is available.

You can find more information about Accepted Manuscripts in the [author guidelines](#).

Please note that technical editing may introduce minor changes to the text and/or graphics, which may alter content. The journal's standard [Terms & Conditions](#) and the ethical guidelines, outlined in our [author and reviewer resource centre](#), still apply. In no event shall the Royal Society of Chemistry be held responsible for any errors or omissions in this Accepted Manuscript or any consequences arising from the use of any information it contains.

A New Rod-Shaped BODIPY-Acetylene Molecule for Solution-Processed Semiconducting Microribbons in N-Channel Organic Field-Effect Transistors

Mehmet Ozdemir,¹ Donghee Choi,² Yunus Zorlu,³ Bunyemin Cosut,³ Hyungsug Kim,²

Choongik Kim*,² and Hakan Usta*¹

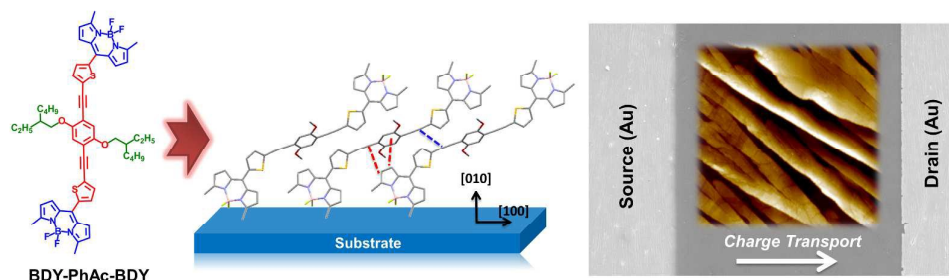
¹ Department of Materials Science and Nanotechnology Engineering, Abdullah Gül University, Kayseri, Turkey

² Department of Chemical and Biomolecular Engineering, Sogang University, Mapo-gu, Seoul, Korea

³ Department of Chemistry, Gebze Technical University, Gebze, Kocaeli, Turkey

*Correspondence to: Prof. Hakan Usta (E-mail:hakan.usta@agu.edu.tr), Prof. Choongik Kim (E-mail: choongik@sogang.ac.kr).

Abstract



BODIPY-based π -conjugated small molecules have been extensively studied in various fields of sensing and biochemical labelling; however, their use in organic optoelectronic applications is very limited. A new solution-processable, acceptor-donor-acceptor (A-D-A) type small molecule, **BDY-PhAc-BDY**, consisting of BODIPY π -acceptors and rod-shaped 1,4-bis-(thienylethynyl)2,5-dialkoxybenzene π -donor, has been synthesized and fully characterized as a novel *n*-channel semiconductor in bottom-gate/top-contact organic field-effect transistors (OFETs). The new semiconductor exhibits an electrochemical band gap of 2.12 eV with highly stabilized HOMO/LUMO energy levels of -5.68 eV/-3.56 eV. Single-crystal X-ray diffraction (XRD) analysis of **BDY-PhAc-BDY** reveals a relatively low “BODIPY-*meso*-thiophene” dihedral angle ($\theta = 44.94^\circ$), antiparallel π -stacked BODIPY dimers with an interplanar distance of 3.93 Å, and strong “C-H $\cdots\pi$ (2.85 Å)” interactions. The OFET devices fabricated by solution processing shows the formation of highly-crystalline, one-dimensional (1-D) microribbons, which results in clear *n*-channel semiconductivity with electron mobility of 0.004 cm²/V·s and the on/off current ratio of 10⁵-10⁶. This is the highest reported to date for BODIPY-based small molecular semiconductors having alkyne linkages. Our results clearly demonstrate that BODIPY is an effective π -acceptor unit for the design of solution-processable, electron-transporting organic semiconductors and easily fabricable 1-D semiconductor micro-/nano-structures for fundamental/applied research in organic optoelectronics.

Introduction

Solution-processable π -conjugated small molecules allow for the fabrication of thin, low-weight, and flexible organic optoelectronic devices such as field-effect transistors (OFETs)¹, light-emitting transistors (OLETs)², and photovoltaics (OPVs)³. They offer significant physical/chemical advantages over their inorganic counterparts including low-cost, compatibility with flexible substrates and roll-to-roll printing process, and structural versatility.⁴⁻⁷ In the past several decades, the major advances in the performances of organic optoelectronic devices have been mainly due to the development of novel semiconducting structures employing properly designed π -architectures and the detailed understanding of their optoelectronic properties.⁸⁻¹⁴ Therefore, the continued research efforts for the search of new semiconductor π -structures and elucidating structure-property-device performance relationships is critical to developing novel optoelectronic platforms with varied functionalities. To this end, 4,4-difluoro-4-bora-3a,4a-diaza-s-indacene (BODIPY) stays as a relatively unexplored π -core for use in semiconductor structures, despite it has been heavily studied in the past decades as highly fluorescent functional dyes for chemosensors, fluorescent switches and biochemical labels.¹⁵ BODIPY is a coplanar and highly electron-deficient π -core with a high dipole moment ($\mu = 3.4-4.2$ D), which makes it an ideal π -acceptor unit to build donor-acceptor type semiconductor architectures.^{16,17} Furthermore, considering its excellent photophysical and photochemical properties, BODIPY-based semiconductors would be ideal functional materials for light-based optoelectronic applications such as OLETs and OPVs.¹⁸ However, to date there has been very few reports on BODIPY-based semiconductor small molecules for optoelectronics with typical charge carrier mobilities of $10^{-5}-10^{-3}$ $\text{cm}^2/\text{V}\cdot\text{s}$.¹⁹ To this end, our recent study revealed that properly designed A-D-A (acceptor-donor-acceptor) molecular π -architectures employing BODIPY acceptor unit can induce n -channel semiconductivity with electron mobilities of up to ~ 0.01 $\text{cm}^2/\text{V}\cdot\text{s}$

and $I_{\text{on}}/I_{\text{off}}$ ratios of 10^7 - 10^8 , which has been the highest performance reported to date for a BODIPY-based semiconductor molecule.²⁰ Motivated with our initial promising findings and to elucidate the full potential of BODIPY π -core in electron-transporting molecules, we are interested in pursuing new BODIPY-based A-D-A π -architectures and exploring their semiconducting characteristics in *n*-channel OFETs.

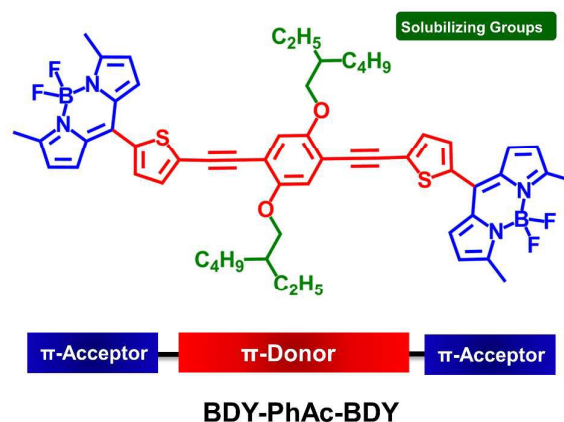


Figure 1. The chemical structure of **BDY-PhAc-BDY** developed in this study indicating donor, acceptor, and solubilizing parts.

In this paper, we report the synthesis, characterization, and field-effect response of a novel *n*-channel semiconductor molecule, **BDY-PhAc-BDY** (Figure 1). In this structure, rod-shaped 1,4-bis-(thienylethynyl)2,5-dialkoxybenzene π -architecture employs 2-ethylhexyloxy electron-donating groups on the central phenyl ring and terminal highly electron-deficient BODIPY π -units. Alkyne linkages are employed between sterically-bulky central phenyl core and thienyl units as a spacer to result in shape-persistent rod-like structure with further extended effective π -conjugation length.²¹ Note that, due to its quasi-cylindrical electronic symmetry, alkyne linkages are advantageous to accommodate steric and conformational constraints.²² The rationale of having BODIPYs linked to five-membered thiophene units from their meso positions is to minimize inter-ring torsions between donor and acceptor units, and to extend π -conjugation along the molecular backbone. Furthermore, 2-ethylhexyloxy lipophilic substituents provide the required solubility in common organic solvents for

convenient purification and thin-film fabrication. Donor-acceptor backbone provides a low optical band gap of 2.2 eV with a relatively stabilized LUMO/HOMO energy level of -3.56/-5.68 eV for unipolar *n*-channel semiconductivity. Single-crystal X-ray diffraction (XRD) analysis shows important structural features about the new semiconductor. The solution-processed **BDY-PhAc-BDY**-based devices exhibit $\mu_e = 0.004 \text{ cm}^2/\text{V}\cdot\text{s}$ with $I_{\text{on}}/I_{\text{off}}$ ratios of 10^5 - 10^6 , which is the highest OFET performance reported so far for BODIPY-based small molecules having alkyne linkages. Detailed morphological and microstructural thin-film analysis reveals the formation of highly-crystalline one-dimensional (1-D) microribbons ([010] in the out-of-plane direction) as a result of favorable “-CH $\cdots\pi$ ” and “ $\pi\cdots\pi$ ” intermolecular interactions. Our results clearly offer crucial guidance for the molecular design of BODIPY-based semiconductor molecules and easily fabricable microribbon-based thin-films for *n*-channel OFETs.

EXPERIMENTAL

Materials and Methods

Schlenk techniques were used in the reactions, and the reactions were carried out under N₂ unless otherwise noted. All reagents were obtained from commercial sources and used without any purification unless otherwise noted. ¹H/¹³C NMR characterizations were performed on a Bruker 400 spectrometer (¹H, 400 MHz; ¹³C, 100 MHz). Elemental analyses were done on a LecoTruspec Micro model instrument. MALDI-TOF was performed on a Bruker Microflex LT MALDI-TOF-MS Instrument. Thermogravimetric analysis (TGA) and differential scanning calorimetry (DSC) measurements were performed on Perkin Elmer Diamond model instruments at a heating rate of 10 °C/min under nitrogen. UV-Vis absorption and fluorescence emission measurements were performed on a Shimadzu, UV-1800 UV-Vis Spectrophotometer and a Varian Eclipse spectrofluorometer, respectively. The fluorescence quantum yield was determined in dichloromethane as compared to the fluorescence of

Rhodamine 6G standart ($\Phi_F = 0.76$ in water). Electrochemistry was performed on a C3 cell stand electrochemical station equipped with BAS-Epsilon software (Bioanalytical Systems, Inc. Lafayette, IN). The molecular geometry optimizations and total energy calculations were carried out using density functional theory (DFT) at the B3LYP/6-31G** level by using Gaussian 09.²³

Synthesis and Characterization

The synthesis of 5-bromo-2-thiophenecarbaldehyde and 2-methylpyrrole reagents were performed in accordance with our previously reported procedures.²⁰

Synthesis of 1,4-dibromo-2,5-bis((2-ethylhexyl)oxy)-2,5-diethynylbenzene (1). A mixture of potassium carbonate (4.0 g, 28.97 mmol) and 2-ethylhexyl bromide (8.24 g, 40.55 mmol) was dissolved in 40 mL DMF under nitrogen. 2,5-dibromohydroquinone (3.88 g, 14.48 mmol) was added slowly to this mixture, and the resulting reaction solution was stirred at 100 °C for 48 h. The mixture was then cooled to room temperature and quenched with water. The reaction mixture was extracted with dichloromethane, and the organic phase was washed with water, dried over Na₂SO₄, filtered, and evaporated to dryness to give the crude product. The crude was then purified by column chromatography on silica gel using hexane as the eluent to give compound **1** as a colorless oil (6.9 g, 97%). ¹H NMR (400 MHz, CDCl₃) δ 7.09 (s, 2H), 3.83 (d, 4H, J=8.0 Hz), 1.76 (m, 2H, J=12.0 Hz), 1.43-1.57 (m, 8H), 1.32-1.35 (m, 8H), 0.91-0.96 (m, 12H). ¹³C NMR (100 MHz, CDCl₃): 150.1, 118.1, 111.0, 72.5, 39.4, 30.4, 29.0, 23.8, 23.0, 14.1, 11.1.

Synthesis of ((2,5-bis((2-ethylhexyl)oxy)-1,4-phenylene)bis(ethyne-2,1-diyl)) bis(trimethylsilane) (2). A mixture of 1,4-dibromo-2,5-bis((2-ethylhexyl)oxy)-2,5-diethynylbenzene (**1**) (2.0 g, 4.06 mmol), Pd(PPh₃)₂Cl₂ (0.171 g, 0.243 mmol), and CuI (0.039 g, 0.203 mmol) in Et₃N (40 mL) was stirred 5 minutes. Next, ethynyltrimethylsilane (1.0 g, 10.16 mmol) was added, and the reaction was heated at 90 °C under nitrogen for 48 h.

Then, the reaction mixture was cooled down to room temperature and filtered; the filtrate was evaporated to dryness to yield a crude. The crude was then purified by column chromatography on silica gel using hexane:ethylacetate (30:1) as the eluent to compound **2** as a yellow oil (1.69 g, 79%). ^1H NMR (400 MHz, CDCl_3) δ 6.89 (s, 2H), 3.81-3.86 (dd, 4H), 1.72-1.75 (m, 2H, $J=12.0$ Hz), 1.44-1.58 (m, 8H), 1.32-1.34 (m, 8H), 0.91-0.96 (m, 12H), 0.26 (s, 18H).

Synthesis of 1,4-bis((2-ethylhexyl)oxy)-2,5-diethynylbenzene (3). The suspension of ((2,5-bis((2-ethylhexyl)oxy)-1,4-phenylene)bis(ethyne-2,1-diyl))bis(trimethylsilane) (**2**) (0.29 g, 0.55 mmol) and KOH (0.93 g, 16.51 mmol) in THF:methanol (9:1) (30 mL) was stirred at room temperature for 1 h. Then, the reaction was quenched with water, and the resulting mixture was extracted with dichloromethane. The organic phase was washed with water, dried over Na_2SO_4 , filtered, and evaporated to dryness to compound **3** as a yellow oil-solid (0.21 g, 100% yield). ^1H NMR (400 MHz, CDCl_3): δ 6.96 (s, 2H), 3.85-3.86 (d, 4H, $J=4.0$ Hz), 3.33 (s, 2H), 1.75-1.78 (m, 2H), 1.46-1.57 (m, 8H), 1.27-1.34 (m, 8H), 0.91-0.96 (m, 12H).

Synthesis of 8-(2-bromothiien-5-yl)-3,5-dimethyl-4,4-difluoro-4-bora-3a,4a-diaza-s-indacene (BDY-Th-Br). Trifluoroacetic acid (TFA) (4 drops) was added to a solution of 5-bromo-2-thiophenecarbaldehyde (0.90 g, 4.70 mmol) and 2-methylpyrrole (0.86 g, 10.64 mmol) in degassed CH_2Cl_2 (300 mL), and the resulting mixture was stirred at room temperature overnight. Next, 2,3-dichloro-5,6-dicyano-1,4-benzoquinone (DDQ) (1.06 g, 4.70 mmol) was added, and the reaction mixture was stirred for additional 2.5 h. Finally, N,N -diisopropylethylamine ($i\text{-Pr}$) $_2\text{EtN}$ (1.33 g, 10.31 mmol) and boron trifluoride diethyl etherate ($\text{BF}_3 \cdot \text{Et}_2\text{O}$) (2.33 g, 16.44 mmol) were added, and the reaction mixture was stirred for additional 2 h. The reaction mixture was poured into water and extracted with CH_2Cl_2 . The organic phase was dried over Na_2SO_4 , filtered, and evaporated to dryness to give a crude product, which was further purified by column chromatography on silica gel using

CH₂Cl₂:Hexanes (2:1) as the eluent. The pure product was obtained as a crystalline red solid (0.78 g, 44% yield). m.p. 132-133 °C. ¹H NMR (400 MHz, CDCl₃): δ 7.18 (m, 2H), 7.05 (d, 2H, J = 4.0 Hz), 6.31 (d, 2H, J=4.0 Hz), 2.66 (s, 6H). ¹³C NMR (100 MHz, CDCl₃): 15.0, 116.9, 119.7, 130.1, 130.6, 131.7, 133.2, 133.9, 136.1, 158.2.

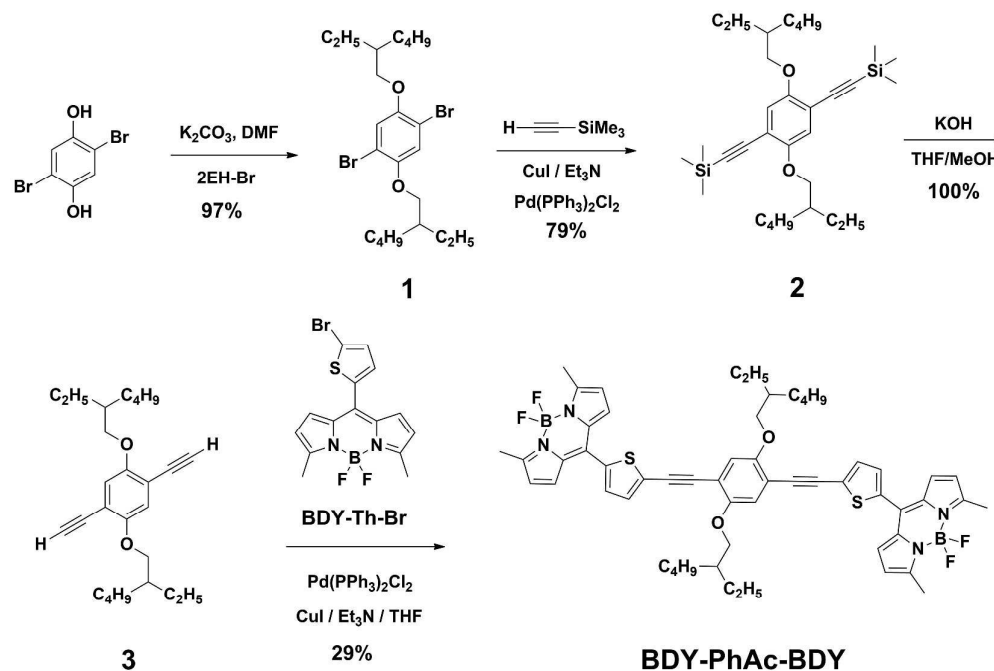
Synthesis of 10-(5-((4-((5-(5,5-difluoro-3,7-dimethyl-5H-4H,5H4-dipyrrolo[1,2-c:2',1'-f][1,3,2]diazaborinin-10-yl)thiophen-2-yl)ethynyl)-2,5-bis((2-ethylhexyl)oxy)phenyl)ethynyl)thiophen-2-yl)-5,5-difluoro-3,7-dimethyl-5H-4H,5H4-dipyrrolo[1,2-c:2',1'-f][1,3,2]diazaborinine (BDY-PhAc-BDY). The reagents 8-(2-bromothien-5-yl)-3,5-dimethyl-4,4-difluoro-4-bora-3a,4a-diaza-s-indacene (**BDY-Th-Br**) (0.675 g, 1.77 mmol), CuI (0.0076 g, 0.040 mmol) and Pd(PPh₃)₂Cl₂ (0.056 g 0.08 mmol) in Et₃N:THF (2:1) (21 mL) were stirred for 5 minutes. Then, 1,4-bis((2-ethylhexyl)oxy)-2,5-diethynylbenzene (**3**) (0.308 g, 0.8 mmol) in 5 mL of THF was added, and the resulting mixture was heated at 80 °C under nitrogen for 24 h. Then, the reaction mixture was cooled to room temperature and evaporated to dryness. The crude was then purified by column chromatography on silica gel using dichloromethane as the eluent to give the pure product as a dark red solid (0.228 g, 29%). ¹H NMR (400 MHz, CDCl₃): δ 7.34 (m, 4H), 7.09 (d, 4H, J= 4.0 Hz), 7.02 (s, 2H), 6.33 (d, 4H, J= 4.0 Hz), 3.94 (m, 4H), 2.67 (s, 12.0 H), 1.80 (m, 2H), 1.52-1.58 (m, 8H), 1.27-1.36 (m, 8H), 0.98 (t, 6H), 0.90 (t, 6H). ¹³C NMR (100 MHz, CDCl₃):δ 158.0, 153.9, 136.0, 134.0, 133.6, 132.0, 131.6, 130.2, 127.9, 119.6, 116.0, 113.7, 93.1, 87.5, 72.0, 39.6, 30.7, 29.1, 24.1, 23.1, 15.0, 14.1, 11.4. m.p. = 196-197 °C. MS(MALDI-TOF) m/z (M⁺): calcd. for C₅₆H₆₀B₂F₄N₄O₂S₂: 982.43, found: 983.302 [M+H]⁺, 963.534 [M-F]⁺, 870.685 [M-1×(2-EH)]⁺, 758.961 [M-2×(2-EH)]⁺. Anal.calcd. for C₅₆H₆₀B₂F₄N₄O₂S₂: C, 68.43; H, 6.15; N, 5.70, Found: C, 68.78; H, 6.25; N, 5.74.

Device Fabrication and Characterization

The OTFTs were fabricated by the bottom-gate/top-contact (BG/TC) structure. Highly n-doped silicon wafers (capacitance per unit area $C_i = 11.4 \text{ nF}\cdot\text{cm}^{-2}$) with thermally oxidized 300 nm SiO_2 layer were cleaned via acetone sonication for 10 min and oxygen plasma cleaning for 5 min (Harrick plasma, PDC-32G, 18 W). The organic layers of BDY-PhAc-BDY were deposited via solution-shearing on PS-brush-treated substrates. The PS-brush ($M_w = 10 \text{ kg/mol}$) treatments were implemented by the general recipe²⁴ and the solution-shearing process was accomplished as the reported procedure.²⁵ The solution-sheared substrates were annealed in a vacuum oven at 100 °C for 24 h to remove the residual solvent. The concentration of BDY-PhAc-BDY solution (1 – 2 mg/mL), solvent type, substrate temperature (50 – 80 % of the solvent boiling point), and shearing speed (0.5 – 8 mm/min) were optimized. The thickness of organic films (40 – 62 nm) were measured by the profilometer (DEKTAK-XT, Brucker). The Au layers (40 nm) with various channel widths (W ; 1000 and 500 μm) and lengths (L ; 100 and 50 μm) were thermally evaporated to define the source and drain electrodes. The electronic performances of OTFTs were characterized in vacuum condition ($<10^{-2}$ Torr) at room temperature with the probe station (Keithely 4200-SCS). The microstructure and surface morphology of thin-films were measured by atomic force microscope (AFM, NX10, Park systems), scanning electron microscope (SEM, JSM-6010LA, JEOL), and X-ray diffraction (XRD, Smartlab, Rigaku).

RESULTS AND DISCUSSIONS

Synthesis, Single-Crystal Structure and Thermal Characterizations

Scheme 1. Synthetic route to **BDY-PhAc-BDY**.

The synthesis of **BDY-PhAc-BDY** is shown in Scheme 1. 2,5-Dibromohydroquinone was first reacted with 2-ethylhexylbromide (2EH-Br) in the presence of K_2CO_3 base in DMF to yield double alkylated product **1** in 97% yield. Double alkyne reaction of **1** was performed via Sonogashira cross-coupling reaction with ethynyltrimethylsilane ($HC\equiv C-SiMe_3$) by using $Pd(PPh_3)_2Cl_2$ catalyst in the presence of CuI/Et_3N . This reaction yielded **2** in 79% yield, which then underwent quantitative (100% yield) desilylation with KOH to form hydrogen-ended ethynyl groups in compound **3**. In the final Sonogashira cross-coupling reaction, **3** was reacted with **BDY-Th-Br** in the presence of $Pd(PPh_3)_2Cl_2$ catalyst and CuI/Et_3N cocatalyst/base mixture. Note that **BDY-Th-Br** was prepared in accordance with our reported procedure.²⁰ Thanks to the good solubility of the target small molecule in common organic solvents, the purification was carried out via column chromatography using $CHCl_3$ as eluent (29% yield). The chemical structure and purity of the intermediate

compounds and the resulting small molecule, **BDY-PhAc-BDY**, were characterized by $^1\text{H}/^{13}\text{C}$ NMR (Figures S1-S6), MALDI-TOF (Figure S7), and Elemental Analysis. Diffraction-quality single-crystals of **BDY-PhAc-BDY** were obtained by diffusion of methanol into a chloroform solution at room temperature, and the corresponding solid-state structure was confirmed by single-crystal X-ray analysis (Figure 2). **BDY-PhAc-BDY** is crystallized in the triclinic space group P-1 and it is located on a crystallographic inversion center. BODIPY frame (C_9BN_2) adopts a nearly coplanar π -structure with the boron atom locating slightly out of this plane by 0.159(10) Å. As shown in Figure 2B, BODIPY π -core shows a dihedral angle (θ_{dihedral}) of 44.94° with the *meso*-thiophene ring, which is slightly lower than our previously reported “BODIPY-Thiophene” dihedral angle (48.80°).²⁰ Moreover, this is much smaller than those measured between the dipyrin framework and the *meso*-phenyl and thienyl units in previously reported BODIPY small molecules ($\theta_{\text{dihedral}} > 54\text{--}90^\circ$).^{19,26–28} This co-planarization reflects the structural advantages of the current π -system including absence of β -pyrrole substitutions and sterically-confined nature of the five-membered thiophene ring.²⁹ The B1–F1 (1.385(11) Å) and B1–F2 (1.378(10) Å) bond distances and F1–B1–F2 ($110.1(7)^\circ$), N1–B1–N2 ($106.8(7)^\circ$), and N–B–F (av. 109.975°) bond angles are similar to those found in the literature.³⁰ As shown in Figure 2C, the detailed crystal packing analysis of **BDY-PhAc-BDY** indicates that the presence of 2-ethylhexyloxy moieties on the central benzene ring prevents the π - π stacking interactions to occur between the complete molecular π -backbones. However, BODIPY π -cores are still found to employ antiparallel arranged, π -stacked dimers with an interplanar distance of 3.93 Å in the unit cell (Figure 2D). This arrangement is most likely a result of the energetically favorable antiparallel dipole-dipole interactions between the BODIPY cores’ strong molecular dipole moments ($\mu = 3.38$ Debye)¹⁷ oriented toward the 4,4'-fluorine substituents. In addition, relatively weaker “ $\pi \cdots \pi$ ” (~ 4.51 Å) interactions were observed between ethynyl ($-\text{C}\equiv\text{C}-$) groups which, in combination with the strong edge-to-face

“C-H $\cdots\pi$ (*dialkoxyphenylic*) ($\sim 2.85\text{\AA}$)” interactions between π -electron-deficient BODIPY-pyrrole hydrogens and the central π -electron-rich dialkoxybenzene ring or ethynyl ($-\text{C}\equiv\text{C}-$) group, is found to play a critical role not only in solid-state formation, but also in thin-film crystallization to form highly crystalline microribbons (Figure 5C, *vide infra*).

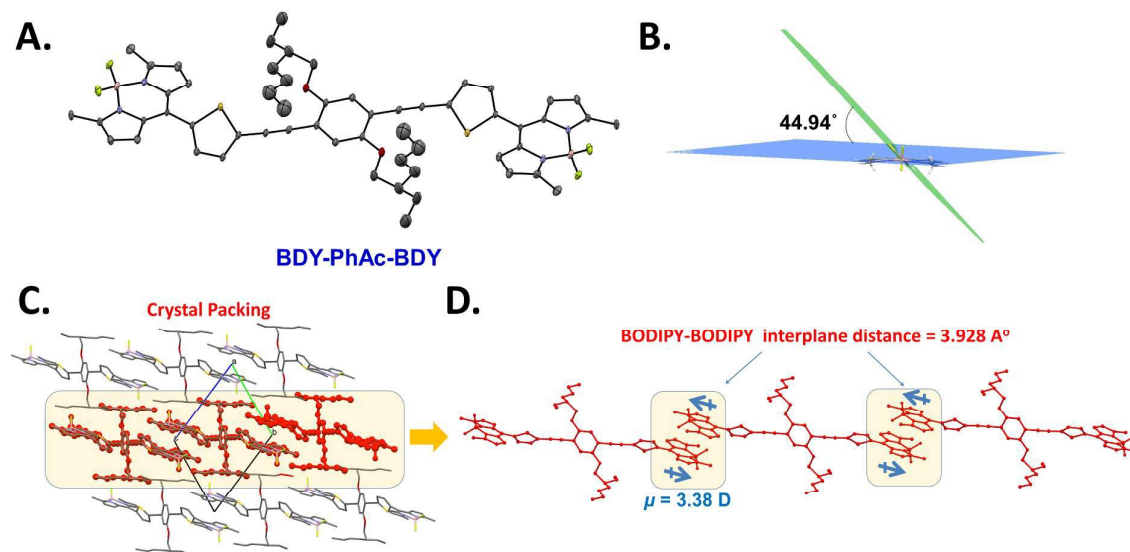


Figure 2. A. X-ray crystal structure of **BDY-PhAc-BDY** with 20% ellipsoids. The grey, blue, red, pink, yellow, and white coloured atoms represent C, N, O, B, F, and H, respectively, B. the perspective view of the inter-ring dihedral angle between boron-dipyrromethene and *meso*-aromatic unit planes, C. Crystal packing of **BDY-PhAc-BDY**, and D. The perspective view of antiparallel arranged, π -stacked dimers (3.928 \AA) occurred between two BODIPY units. The local dipole moments ($\mu = 3.38$ Debye) of BODIPY cores are shown in blue.

As shown in Figure 3, **BDY-PhAc-BDY** was found to be highly thermally stable with the thermolysis onset temperature (5% mass loss) located at $300\text{ }^\circ\text{C}$. A two-step decomposition behavior was observed with a small step at $\sim 87\%$ of the original weight, corresponding to the mass loss of one of the alkyl substituents ($-\text{CH}_2\text{CH}(\text{C}_2\text{H}_5)(\text{C}_4\text{H}_9)$). Differential scanning calorimetry (DSC) measurement shows a sharp endothermic peak at $198\text{ }^\circ\text{C}$ with an enthalpy of 62.65 J/g . This peak indicates the thermal transition of the crystalline **BDY-PhAc-BDY** solid into an isotropic liquid, which was further confirmed by conventional melting-

temperature measurement ($T_{m.p.} = 196\text{-}197\text{ }^{\circ}\text{C}$). This is very different from our previously reported non-substituted BODIPY-small molecules, **BDY-3T-BDY/BDY-4T-BDY**, which have showed thermal decompositions with no observable melting points.²⁰ This reflects the critical role of flexible swallow-tailed 2-ethylhexyloxy substituents to tune intermolecular interactions, which eventually induces melting process. Note that once the crystalline solid obtained from chromatographic purification melts to an isotropic liquid, no corresponding crystallization peak was observed in the cooling cycle. This indicates that **BDY-PhAc-BDY** adopts an amorphous solid-state upon cooling and it does not exhibit further melting peak in the second-heating cycle (Figure 3B).

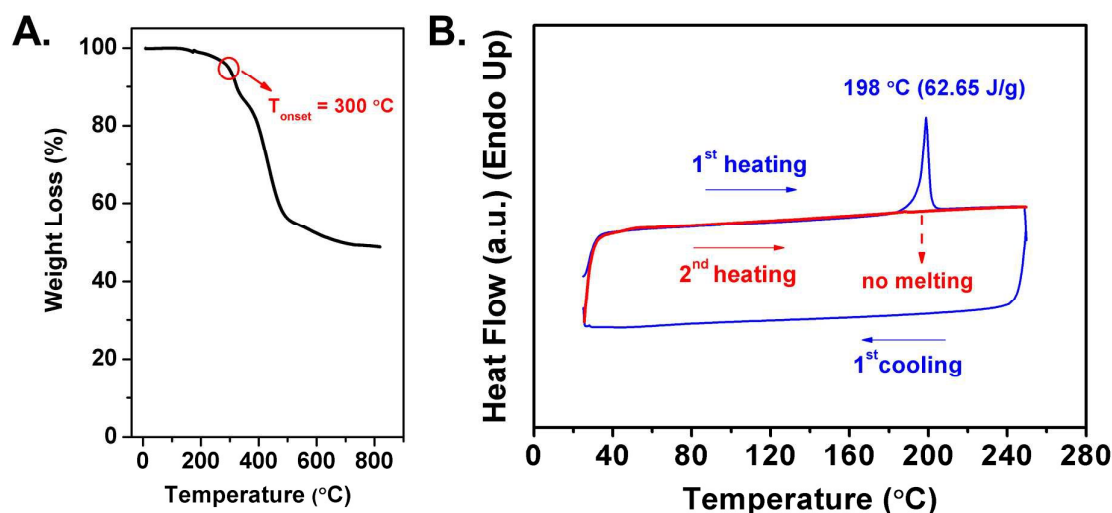


Figure 3. A. Thermogravimetric analysis (TGA), and B. Differential scanning calorimetry (DSC) measurement curves of **BDY-PhAc-BDY** at a temperature ramp of $10\text{ }^{\circ}\text{C}/\text{min}$ under N_2 .

Optical and Electrochemical Properties

The electrochemical and optical properties of **BDY-PhAc-BDY** were evaluated by UV-vis absorption and photoluminescence spectroscopies, and cyclic voltammetry. **BDY-PhAc-BDY** exhibits two absorption peaks in dichloromethane solution with λ_{max} located at 355 nm and 527 nm. The large molar extinction coefficient ($\epsilon = 1 \times 10^5\text{ M}^{-1}\text{ cm}^{-1}$) for the absorption peak

at 527 nm and the out-of-plane vibronic feature at 495 nm ($\sim 1200 \text{ cm}^{-1}$ shift from λ_{max}) are unique features of the BODIPY-based $\pi\text{-}\pi^*$ ($S_0 \rightarrow S_1$) transition.¹⁵ The broad peak with lower intensity at 355 nm is ascribed to a combination of BODIPY-based $S_0 \rightarrow S_2$ and 1,4-bis-(thienylethynyl)2,5-dialkoxybenzene-based $\pi\text{-}\pi^*$ transitions. The optical band gap is estimated as 2.22 eV from the low-energy absorption edge. In the thin-film state (spin-coated on glass substrate), the absorption maxima show bathochromic shifts ($\lambda_{\text{max}} = 365/543 \text{ nm}$) and the optical band gap is lowered to 2.06 eV (solid-state) with respect to those in the solution. This is indicative of molecular π -backbone planarization and solid-state ordering as compared to the solution phase. The fluorescence spectrum of **BDY-PhAc-BDY** in dichloromethane solution (Figure S8) exhibits a broad emission peak with a largely shifted maxima of 646 nm (Stokes shift = 119 nm) and a very low quantum yield (Φ_{F}) of $\sim 0.02\%$. This is very different from typical BODIPY emission features such as high quantum yield and extremely low Stokes shifts, and it reflects most likely the presence of nonradiative pathways in the excited state via intra-/inter-molecular charge transfer processes.³¹ When the solvent dielectric constant is lowered (THF ($\epsilon = 8.9$) \rightarrow toluene ($\epsilon = 2.3$)), a highly blue-shifted PL spectra was measured in toluene (Figure S8, $\lambda_{\text{em}} = 578 \text{ nm}$) indicating positive solvachromatism. This further confirms that the final relaxed excited state employs a large dipole moment as a result of charge transfer (CT) between subchromophoric units. Based on the DFT calculations (B3LYP/6-31G** level of theory), lowest unoccupied molecular orbital (LUMO) of **BDY-PhAc-BDY** is found to be symmetrically localized on the outer BODIPY π -acceptor units, while highest occupied molecular orbital (HOMO) is delocalized only on the central π -donor part with noticeable contributions from the oxygens on the alkoxy groups (Figure 4-inset). This further supports the emission characteristics of **BDY-PhAc-BDY**, that the photoexcitation is probably accompanied with an intramolecular charge-transfer (CT) in the excited state from donor to acceptor unit (HOMO \rightarrow LUMO). Cyclic voltammetry

measurements reveal two reversible reductions and one quasi-reversible oxidation for **BDY-PhAc-BDY** with the first half-wave reduction-potential ($E_{1/2}^{\text{red-1}}$) located at -0.84 V and the first onset oxidation-potential ($E_{\text{onset}}^{\text{ox-1}}$) located at 1.28 V. The electrochemical band gap (2.12 eV) shows excellent agreement with the optical band gap (2.22 eV) measured in solution. The HOMO and LUMO energy levels are estimated as -5.68 eV and -3.56 eV, respectively. Note that, as a result of π -electron deficiency of the *meso*-substituted BODIPY's at the molecular termini, LUMO energy level of the new molecule is sufficiently stabilized to be in the energetic range of previously reported *n*-channel semiconductors (-2.9 to -4.3 eV).³² Furthermore, when compared with the observed *p*-doping characteristics, highly reversible and favorable reductive properties of **BDY-PhAc-BDY** are indicative of its electron-transporting semiconductor potential.

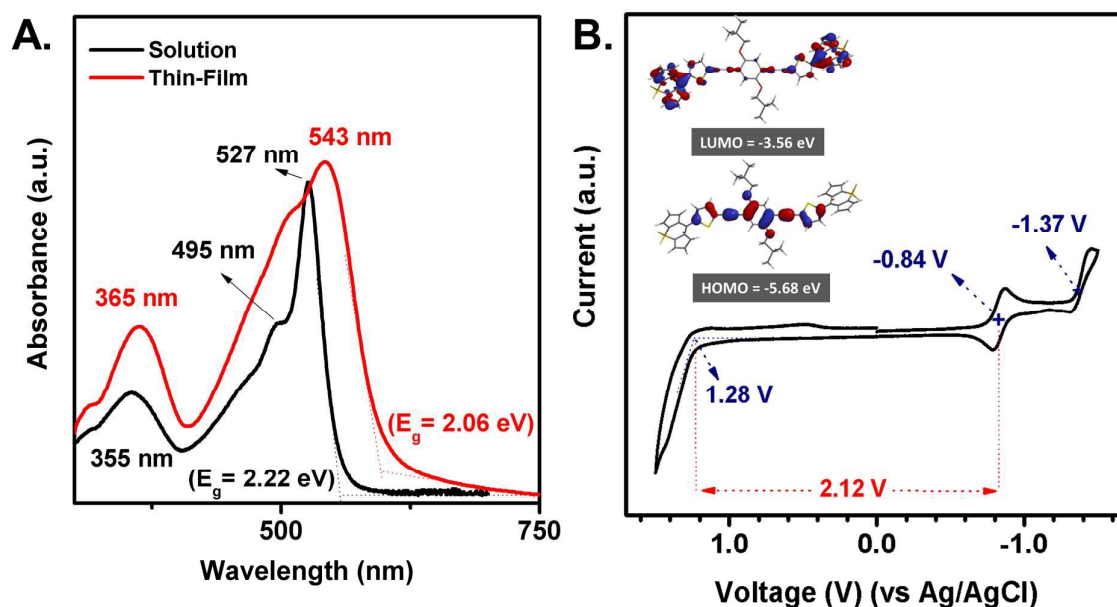


Figure 4. A. Optical absorption in dichloromethane solution (black line) and as thin-film (red line) of **BDY-PhAc-BDY**, and B. Cyclic voltammogram of **BDY-PhAc-BDY** in dichloromethane (0.1M $\text{Bu}_4\text{N}^+\text{PF}_6^-$, scan rate = 50 $\text{mV}\cdot\text{s}^{-1}$). Inset shows the calculated (DFT, B3LYP/6-31G**) topographical orbital representations and experimentally estimated HOMO and LUMO energy levels.

Thin-Film Microstructure/Morphology and Field-Effect Transistor Characterization

The semiconductor thin-films (40-62 nm) were fabricated by solution-shearing **BDY-PhAc-BDY** solution in 1,2,4-trichlorobenzene (1.0 mg/mL) on PS (polystyrene)-brush treated n^{++} -Si/SiO₂ substrates. Bottom-gate/top-contact (BG/TC) OFETs were completed by thermal evaporation of source and drain Au electrodes (40 nm) via thermal evaporation (deposition rate = 0.2 Å/s) to yield various channel lengths (L: 100 and 50 μm) and widths (W: 1000 and 500 μm). The microstructure of solution-sheared **BDY-PhAc-BDY** thin-film was investigated by out-of-plane X-ray diffraction measurement, which displays a major diffraction peak at $2\theta = 8.94^\circ$ (Figure 5A). The second and third order diffractions of the same crystalline phase were also observed revealing a high degree of ordering across the thin-film thickness. The simulation of the powder pattern based on the single-crystal structure of **BDY-PhAc-BDY** (Figure S9) shows that all these peaks are well indexed along the (010) lattice plane, and second and third order diffractions correspond to (020) and (030), respectively. The periodicity (*d*-spacing) of the (010) plane in thin-film phase is measured as 9.88 Å, which corresponds to “*b*-axis (10.928 Å) × sin α (66.26°)” and suggests that the molecules are adopting a highly tilted molecular orientation on the substrate (Figure 5C). Atomic force microscopy (AFM) and scanning electron microscopy (SEM) characterizations show that the morphology of the solution-sheared thin-film of **BDY-PhAc-BDY** consists of one-dimensional (1-D) highly crystalline micron-sized ribbons, which are perfectly aligned along the shearing direction (Figure 5B). The lengths of the microribbons can reach to ~0.1 mm and their widths were ~0.5-2.0 μm. Detailed analysis of the AFM image also shows the formation of well-connected smaller grains having ~200-500 nm lengths along the ribbon long-axis. In order to elucidate the structural packing in these micro-ribbons, the BFDH (Bravais, Friedel, Donnay, and Harker) theoretical crystal morphology was used, which predicts a high aspect ratio crystal growth perpendicular to the [010] out-of-plane direction. Since the self-assembly

process during thin-film crystallization may be similar to single-crystal formation, the thermodynamically/kinetically more favored primary crystal growth along the [100] crystallographic direction most likely reflects the anisotropic ribbon growth due to similar directional intermolecular forces.^{33–35} This shows that the major intermolecular interactions governing the thin-film crystallization are: (i) strong “-CH \cdots π ” contacts ($\sim 2.85\text{\AA}$) between π -deficient BODIPY-pyrrole hydrogens and the central π -electron rich dialkoxybenzene ring/ethynyl (-C \equiv C-) groups, (ii) “ $\pi\cdots\pi$ ” ($\sim 4.5\text{\AA}$) interactions between ethynyl (-C \equiv C-) groups, and (iii) “ $\pi\cdots\pi$ ” ($\sim 3.9\text{\AA}$) and dipole-dipole interactions between antiparallel arranged BODIPY frameworks (*vide infra*). It appears to us that also the directional solution-shearing process used for the current thin-film fabrications might play a key role to facilitate **BDY-PhAc-BDY**'s molecular self-assembly into anisotropic ribbons along the shearing direction.²⁵ The formation of ribbon-like morphology with the solution-shearing method is consistent with our previous rod-like BODIPY small molecules (**BDY-3T/4T-BDY**) which has also yielded high-aspect ratio microfibers in thin-film.

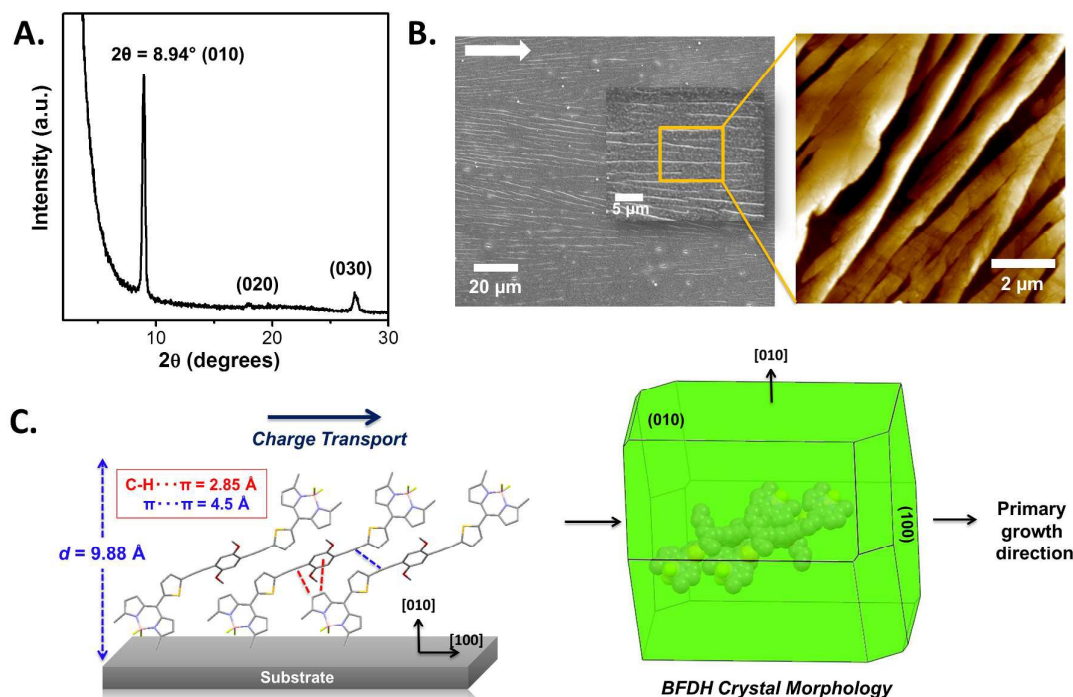


Figure 5. θ - 2θ X-ray diffraction (XRD) scans (A) and SEM/AFM-topographic images (B) of solution-sheared **BDY-PhAc-BDY** thin-film. (C) The molecular arrangement in the out-of-plane [010] direction and the BFDH (Bravais, Friedel, Donnay and Harker) theoretical crystal morphology showing the primary crystal growth direction ([100]). The arrow shows the shearing direction. “-CH $\cdots\pi$ ” contacts ($\sim 2.85\text{\AA}$) and “ $\pi\cdots\pi$ ” ($\sim 4.5\text{\AA}$) interactions are shown between two representative molecules.

OFET device characteristics were measured with a Keithley 4200-SCS semiconductor characterization system at room temperature. The transistor characteristics in the saturation regime such as charge carrier mobilities (μ) and threshold voltages (V_T) were extracted from the equation:

$$\mu_{\text{sat}} = (2I_{\text{DS}}L) / [WC_i(V_G - V_T)^2]$$

where I_{DS} is the drain current, L and W are the channel length and width, respectively, C_i is the areal capacitance of the gate dielectric, V_G is the gate voltage, and V_T is the threshold voltage. Typical transfer and output curves are shown in Figures 6 and S10. Consistent with the theoretical and experimental optoelectronic characterizations on the small molecule (*vide supra*), these devices exhibited n -channel behavior with $\mu_e = 0.004 \text{ cm}^2/\text{V}\cdot\text{s}$ and $I_{\text{on}}/I_{\text{off}} = 10^5$ -

10^6 . This clearly shows that BODIPY is an effective π -acceptor unit to afford a substantial lowering of the LUMO level and to induce n -channel semiconductivity in π -conjugated small molecules for use in optoelectronic devices. Although the current electron mobility for **BDY-PhAc-BDY** thin-film is much lower than the state-of-the-art performances achieved previously with other molecular π -systems, it is still remarkable from a molecular design perspective since it is the highest reported to date for a BODIPY-based small molecular semiconductor having alkyne linkages. Besides, the growth of well-oriented micro- and nano-sized organic semiconductor structures from solution phase has always been challenging in the literature and it offers great advantages in fabricating transistor arrays for circuit design.^{34,36} Although π - π stacking between whole molecular skeletons are not evident along the charge-transport (in-plane) direction, the localized π - π stackings between individual acceptor or donor units in the twisted arrangement of A-D-A π -architecture,³⁷ and strong “-CH $\cdots\pi$ ” interactions in the face-to-edge herringbone packing may still contribute to 3-D charge transport, which, along with the highly-crystalline microstructure, explains the observed mobility. Since the thin-film crystallinity and morphology of the current semiconductor remains similar to our previously reported non-substituted semiconductor, **BDY-4T-BDY**, the slightly reduced (2.5 \times) OFET performance is most likely related to the presence of σ -insulating alkyl substituents on the central benzene ring. Based on our findings, note that BODIPY π -core offers unique advantage by providing good solubility to the molecular π -system even in the absence of alkyl substituent. Therefore, for the future development of solution-processable BODIPY-based semiconductors, we rationalize that non-substituted systems should be preferred to yield higher mobilities.

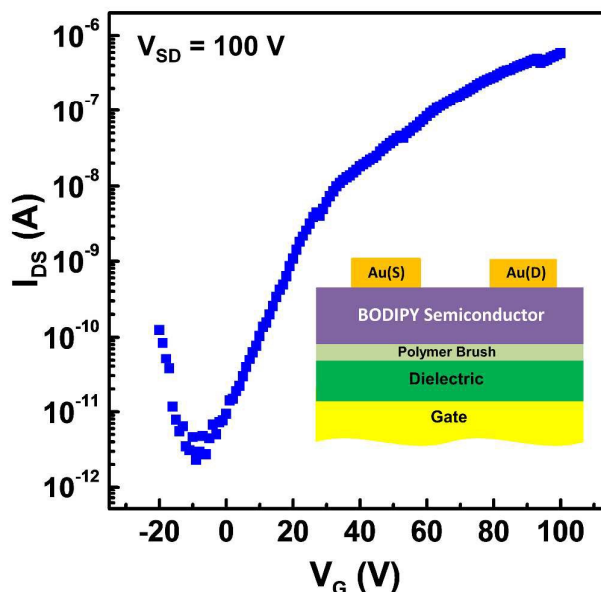


Figure 6. Representative transfer plot in the *n*-channel region for bottom-gate/top-contact (BG/TC) OFET devices fabricated with solution-sheared **BDY-PhAc-BDY** thin-film.

Conclusions

A new solution-processable BODIPY-Acetylene small molecule, **BDY-PhAc-BDY**, based on A-D-A π -architecture was designed, synthesized and fully characterized. The new semiconductor exhibited a low solid-state optical band gap of 2.06 eV with stabilized HOMO and LUMO energy levels of -5.68 eV and -3.56 eV. Single-crystal X-ray diffraction (XRD) analysis reveals crucial structural features and intermolecular interactions such as relatively low “BODIPY-*meso*-thiophene” dihedral angle ($\theta_{\text{dihedral}} = 44.94^\circ$) and antiparallel π -stacked BODIPY dimers with an interplanar distance of 3.93 Å. Highly crystalline one-dimensional (1-D) microribbons of **BDY-PhAc-BDY** were grown from the chloroform solution on PS (polystyrene)-brush treated substrates via solution-shearing method. Strong edge-to-face “C-H(*pyrrolic*) $\cdots\pi$ (*dialkoxyphenylic*) ($\sim 2.85\text{Å}$)” and relatively weaker “ π (*ethynyl*) $\cdots\pi$ (*ethynyl*)” ($\sim 4.51\text{Å}$) directional interactions are found to be effective in the formation of current highly crystalline microribbons along the [100] direction. The bottom-gate/top-contact OFET devices based on these microribbons exhibited clear *n*-channel operation and afforded

electron mobility of $0.004 \text{ cm}^2/\text{V}\cdot\text{s}$ and the on/off current ratio of 10^5 - 10^6 , which is the highest reported till now for BODIPY-based small molecular semiconductors with alkyne linkages. Our findings clearly demonstrate that BODIPY is an effective π -acceptor unit to realize solution-processable donor-acceptor type small molecules for electron-transport. Here, we also offer crucial guidance for the design of future BODIPY-based semiconductor molecules with further improved electrical performances and also easily fabricable 1-D semiconductor thin-film morphologies for fundamental/applied research in organic optoelectronics.

Acknowledgement

H. U. acknowledges support from TUBITAK 114M226. H. U. acknowledges support from Turkish Academy of Sciences, The Young Scientists Award Program (TUBA-GEBİP 2015). C. K. acknowledges support from Basic Science Research Program through the National Research Foundation of Korea (NRF) (NRF-2014R1A1A1A05002158).

Supporting Information

SI includes Figures S1-S7 ($^1\text{H}/^{13}\text{C}$ NMR spectra and MALDI-TOF spectra for the intermediate compounds and the final small molecule), Figure S8 (PL spectra of BDY-PhAc-BDY), Figure S9 (Simulated XRD powder pattern of BDY-PhAc-BDY), and Figure S10 (output plot for the OFET devices). Table S1 and CCDC 1482958 (for **BDY-PhAc-BDY**) contains the supplementary crystallographic data for this paper. These data can be obtained free of charge from The Cambridge Crystallographic Data Centre via www.ccdc.cam.ac.uk/data_request/cif.

References

- 1 H. Ebata, T. Izawa, E. Miyazaki, K. Takimiya, M. Ikeda, H. Kuwabara and T. Yui, *J. Am. Chem. Soc.*, 2007, **129**, 15732–15733.
- 2 R. Capelli, S. Toffanin, G. Generali, H. Usta, A. Facchetti and M. Muccini, *Nat. Mater.*, 2010, **9**, 496–503.
- 3 A. Facchetti, *Chem. Mater.*, 2011, **23**, 733–758.
- 4 J. Li, Y. Zhao, H. S. Tan, Y. Guo, C.-A. Di, G. Yu, Y. Liu, M. Lin, S. H. Lim, Y. Zhou, H. Su and B. S. Ong, *Sci. Rep.*, 2012, **2**, 754.
- 5 H. E. Katz, Z. Bao and S. L. Gilat, *Acc. Chem. Res.*, 2001, **34**, 359–369.
- 6 L. Chua, J. Zaumseil, J. Chang, E. C.-W. Ou, P. K.-H. Ho, H. Sirringhaus and R. H. Friend, *Nature*, 2005, **434**, 194–9.
- 7 M.-C. Chen, S. Vegiraju, C.-M. Huang, P.-Y. Huang, K. Prabakaran, S. L. Yau, W.-C. Chen, W.-T. Peng, I. Chao, C. Kim and Y.-T. Tao, *J. Mater. Chem. C*, 2014, **2**, 8892–8902.
- 8 S. Allard, M. Forster, B. Souharce, H. Thiem and U. Scherf, *Angew. Chemie - Int. Ed.*, 2008, **47**, 4070–4098.

- 9 M. Sawamoto, M. J. Kang, E. Miyazaki, H. Sugino, I. Osaka and K. Takimiya, *ACS Appl. Mater. Interfaces*, 2016, **8**, 3810–3824.
- 10 R. Ponce Ortiz, H. Herrera, M. J. Mancheño, C. Seoane, J. L. Segura, P. Mayorga Burrezo, J. Casado, J. T. López Navarrete, A. Facchetti and T. J. Marks, *Chem. - A Eur. J.*, 2013, **19**, 12458–12467.
- 11 L. Zhang, A. Fonari, Y. Liu, A.-L. M. Hoyt, H. Lee, D. Granger, S. Parkin, T. P. Russell, J. E. Anthony, J.-L. Brédas, V. Coropceanu and A. L. Briseno, *J. Am. Chem. Soc.*, 2014, **136**, 9248–9251.
- 12 M. Durso, C. Bettini, A. Zanelli, M. Gazzano, M. G. Lobello, F. De Angelis, V. Biondo, D. Gentili, R. Capelli, M. Cavallini, S. Toffanin, M. Muccini and M. Melucci, *Org. Electron.*, 2013, **14**, 3089–3097.
- 13 K.-H. Kim, H. Yu, H. Kang, D. J. Kang, C.-H. Cho, H.-H. Cho, J. H. Oh and B. J. Kim, *J. Mater. Chem. A*, 2013, **1**, 14538.
- 14 H. Yu, H.-H. Cho, C.-H. Cho, K.-H. Kim, D. Y. Kim, B. J. Kim and J. H. Oh, *ACS Appl. Mater. Interfaces*, 2013, **5**, 4865–4871.
- 15 A. C. Benniston, G. Copley, A. Harriman and R. Ryan, *J. Mater. Chem.*, 2011, **21**, 2601.
- 16 A. Bessette and G. S. Hanan, *Chem. Soc. Rev.*, 2014, **43**, 3342.
- 17 H. Usta, M. D. Yilmaz, A. J. Avestro, D. Boudinet, M. Denti, W. Zhao, J. F. Stoddart and A. Facchetti, *Adv. Mater.*, 2013, **25**, 4327–4334.
- 18 A. M. Poe, A. M. Della Pelle, A. V Subrahmanyam, W. White, G. Wantz and S. Thayumanavan, *Chem. Commun.*, 2014, **50**, 2913.
- 19 T. Bura, N. Leclerc, S. Fall, P. Lévêque, T. Heiser, P. Retailleau, S. Rihn, A. Mirloup and R. Ziessel, *J. Am. Chem. Soc.*, 2012, **134**, 17404–17407.
- 20 M. Ozdemir, D. Choi, G. Kwon, Y. Zorlu, B. Cosut, H. Kim, A. Facchetti, C. Kim and H. Usta, *ACS Appl. Mater. Interfaces*, 2016, **8**, 14077–14087.
- 21 F. Silvestri, A. Marrocchi, M. Seri, C. Kim, T. J. Marks, A. Facchetti and A. Taticchi, *J. Am. Chem. Soc.*, 2010, **132**, 6108–6123.
- 22 F. Diederich, P. J. Stang and R. R. Tykwinski, Eds., *Acetylene Chemistry: Chemistry, Biology and Materials Science*, Wiley-VCH: Weinheim, 2005.
- 23 Gaussian 09, Revision C.01, M. J. Frisch, G. W. Trucks, H. B. Schlegel, G. E. Scuseria, M. A. Robb, J. R. Cheeseman, G. Scalmani, V. Barone, B. Mennucci, G. A. Petersson, H. Nakatsuji, M. Caricato, X. Li, H. P. Hratchian, A. F. Izmaylov, J. Bloino, G. Zheng, J. L. Sonnenberg, M. Hada, M. Ehara, K. Toyota, R. Fukuda, J. Hasegawa, M. Ishida, T. Nakajima, Y. Honda, O. Kitao, H. Nakai, T. Vreven, J. A. Montgomery, Jr., J. E. Peralta, F. Ogliaro, M. Bearpark, J. J. Heyd, E. Brothers, K. N. Kudin, V. N. Staroverov, T. Keith, R. Kobayashi, J. Normand, K. Raghavachari, A. Rendell, J. C. Burant, S. S. Iyengar, J. Tomasi, M. Cossi, N. Rega, J. M. Millam, M. Klene, J. E. Knox, J. B. Cross, V. Bakken, C. Adamo, J. Jaramillo, R. Gomperts, R. E. Stratmann, O. Yazyev, A. J. Austin, R. Cammi, C. Pomelli, J. W. Ochterski, R. L. Martin, K. Morokuma, V. G. Zakrzewski, G. A. Voth, P. Salvador, J. J. Dannenberg, S. Dapprich, A. D. Daniels, O. Farkas, J. B. Foresman, J. V. Ortiz, J. Cioslowski, and D. J. Fox, Gaussian, Inc., Wallingford CT, 2010.
- 24 S. H. Park, H. S. Lee, J.-D. Kim, D. W. Breiby, E. Kim, Y. D. Park, D. Y. Ryu, D. R. Lee and J. H. Cho, *J. Mater. Chem.*, 2011, **21**, 15580.
- 25 G. Giri, E. Verploegen, S. C. Mannsfeld, S. Atahan-Evrenk, H. Kim do, S. Y. Lee, H. A. Becerril, A. Aspuru-Guzik, M. F. Toney and Z. Bao, *Nature*, 2011, **480**, 504.
- 26 P. E. Kesavan, S. Das, M. Y. Lone, P. C. Jha, S. Mori and I. Gupta, *Dalt. Trans.*, 2015, **44**, 17209–17221.
- 27 H. L. Kee, C. Kirmaier, L. Yu, P. Thamyongkit, W. J. Youngblood, M. E. Calder, L.

- Ramos, B. C. Noll, D. F. Bocian, W. R. Scheidt, R. R. Birge, J. S. Lindsey and D. Holten, *J. Phys. Chem. B*, 2005, **109**, 20433–20443.
- 28 A. C. Benniston, G. Copley, A. Harriman, D. B. Rewinska, R. W. Harrington and W. Clegg, *J. Am. Chem. Soc.*, 2008, **130**, 7174–7175.
- 29 Y. Yang, Q. Guo, H. Chen, Z. Zhou, Z. Guo and Z. Shen, *Chem. Commun.*, 2013, **49**, 3940.
- 30 D. Aydın Tekdaş, G. Viswanathan, S. Zehra Topal, C. Y. Looi, W. F. Wong, G. Min Yi Tan, Y. Zorlu, A. G. Gürek, H. B. Lee and F. Dumoulin, *Org. Biomol. Chem.*, 2016, **14**, 2665–2670.
- 31 M. T. Whited, N. M. Patel, S. T. Roberts, K. Allen, P. I. Djurovich, S. E. Bradforth and M. E. Thompson, *Chem. Commun.*, 2012, **48**, 284–286.
- 32 H. Usta, A. Facchetti and T. J. Marks, *Acc. Chem. Res.*, 2011, **44**, 501–510.
- 33 G. K. Veits, K. K. Carter, S. J. Cox and A. J. McNeil, *J. Am. Chem. Soc.*, 2016, **138**, 12228–12233.
- 34 M. Wang, J. Li, G. Zhao, Q. Wu, Y. Huang, W. Hu, X. Gao, H. Li and D. Zhu, *Adv. Mater.*, 2013, **25**, 2229–2233.
- 35 T. He, M. Stolte and F. Würthner, *Adv. Mater.*, 2013, **25**, 6951–6955.
- 36 H. Li, B. C.-K. Tee, J. J. Cha, Y. Cui, J. W. Chung, S. Y. Lee and Z. Bao, *J. Am. Chem. Soc.*, 2012, **134**, 2760–2765.
- 37 M. Gsänger, J. H. Oh, M. Könemann, H. W. Höffken, A.-M. Krause, Z. Bao and F. Würthner, *Angew. Chemie Int. Ed.*, 2010, **49**, 740–743.